Deformation and Collapse of Zircaloy Fuel Rod Cladding Into Plenum Axial Gaps

P.L. Pfennigwerth, D.A. Gorscak, I.A. Selsley

Westinghouse Electric Corporation, Bettis Atomic Laboratory, P.O. Box 79, West Mifflin, Pennsylvania 15122-0079, U.S.A.

ABSTRACT

To minimize support structure, blanket and reflector fuel rods of the thoria urania-fueled Light Water Breeder Reactor (LWBR) were designed with non-freestanding Zircaloy-4 cladding. An analytical model was developed to predict deformation of unirradiated cladding into axial gaps of fuel rod plenum regions where it is unsupported.

This model uses the ACCEPT finite element computer program to calculate elastic-plastic deformation of cladding due to external pressure. The finite element is 20-node, tri-quadratic, isoparametric, and 3-dimensional. Its curved surface permits accurate modeling of the tube geometry, including geometric nonuniformities such as circumferential wall thickness variation and initial tube out-of-roundness. Progressive increases in axial gap length due to cladding elongation and fuel stack shrinkage are modeled, as are deformations of fuel pellets and stainless steel support sleeves which bound plenum axial gaps in LWBR type blanket fuel rods.

Zircaloy-4 primary and secondary thermal creep representations were developed from uniaxial creep testing of fuel rod tubing. Creep response to multi-axial loading is modeled with a variation of Hill's formulation for anisotropic materials. Coefficients accounting for anisotropic thermal creep in Zircaloy-4 tubes were developed from creep testing of externally pressurized tubes having fixed axial gaps in the range 2.5 cm to 5.7 cm and radial clearances over simulated fuel pellets ranging from zero to 0.089 mm.

Qualification of the analysis procedure is based upon comparisons between predicted and measured ovalities of additional externally pressurized tubing specimens with variable axial gaps that were incrementally increased from 1.3 cm to 4.2 cm to simulate progressive growth of fuel rod plenum gaps during reactor operation. Key geometry parameters were found to be cladding thickness, axial gap length, and radial pellet-cladding clearance. Both analysis and tests indicate that cladding deformation over plenum axial gaps is insensitive to initial tubing out-of-roundness. For axial gap lengths up to about 2.5 cm, initially pre-flattened variable gap specimens became more round with exposure and then, as axial gaps were lengthened, reversed their trend and begin to flatten.

In addition, variable axial gap specimens were found to be more stable than specimens with fixed axial gaps and comparable radial clearances. This behavior resulted from the stabilizing effect of radial clearance decrease from tube diameter shrinkage during early exposure while axial gaps were short. The stabilizing effect was found to persist even after axial gaps were lengthened beyond values found to be unstable in fixed axial gap specimens.

A sample calculation is presented that demonstrates the analysis procedure for a hypothetical fuel rod. Results of the study illustrate that variations between best estimate parameters and conservative limits used for design purposes can produce large differences in performance predictions. For example, the best estimate model predicted negligibly small cladding deformations of the hypothetical fuel rod, whereas the design basis model predicted collapse over the 32-month lifetime analyzed. The sample analysis also illustrates the significant reduction in cladding deformation rates that can result from reductions in system pressure and cladding temperature.

1. Introduction

Blanket and reflector fuel rods of the thoria-urania (^{233}U) fueled Light Water Breeder Reactor (LWBR) [1] have Zircaloy-4 cladding which is designed to creep down onto fuel pellets during reactor operation. Unlike pre-pressurized fuel rods now used in commercial LWR's, LWBR fuel rods were backfilled with helium at only atmospheric pressure. Thus, although potential ballooning during a late in life loss of coolant pressure accident would be mitigated by low internal fuel rod pressures, creep deformation into potential axial gaps during normal sustained operation was a design concern which required particular attention.

Each LWBR blanket and reflector fuel rod was fabricated with a small axial gap (1.3-cm nominal length) to provide space between the fuel stack and a stainless steel plenum sleeve for differential thermal expansion between fuel and cladding. During core life, cladding elongates due to pellet-cladding interaction and due to irradiation growth, and the fuel stack shortens due to fuel densification. The net effect is growth of the initially small plenum axial gap to a predicted maximum length of 5 cm late in life.

Deformation of cladding over plenum gaps at the tops of LWBR blanket and reflector fuel rods is partly elastic and partly inelastic (thermal creep). (Neutron flux in plenum regions of these fuel rods is too small to produce any significant radiation-induced creep.) Load on the cladding is primarily from external primary system pressure. Because LWBR fuel rods were not pre-pressurized and because fission gas release is very low from LWBR thoria-base fuel [2], internal pressure support is negligible.

Experimental and analytical development programs were conducted to provide capability for detailed prediction of cladding deformation over axial gaps in plena of LWBR fuel rods to and beyond the design lifetime of 18,000 effective full power hours. Available analysis programs, e.g., COVE-1 [3], a program prepared by BNWL for the NRC, did not provide the detailed modeling capability required for LWBR application; and available experimental work, e.g., that of Hobson at ORNL [4], Stehle, et al at KWU [5], and Murty, et al at B&W [6,7], did not relate specifically to tubing having LWBR fabrication parameters.

The purpose of this paper is to present correlated results from the LWBR DECAG (Deformation of Cladding into Axial Gaps) thermal creep test program [8 - 10] using the ACCEPT three-dimensional finite element computer program [11] and the LWBR analysis procedure [12].

2. Thermal Creep Test Program

In the first phase of the LWBR thermal creep test program, load controlled, uniaxial tensile creep tests of Zircaloy-4 tubing provided data for thermal creep modeling. In the second phase, externally pressurized Zircaloy-4 tubing was tested in autoclave environments and in geometries relevant to LWBR blanket and reflector fuel rod plena. Both phases of the test program built upon earlier work [13] on Zircaloy-4 tubing which had been performed in support of the LSBR/LWB fuel element development program which preceded LWBR. Tubing tested was either excess production tubing from lots actually used in LWBR fuel rods [14] or pre-production tubing having similar cold working and heat treatment. All tubing was stress relief annealed at 496 ± 13.8°C for 6 hours following final area reduction (60 to 75%).

The thermal creep model used in the ACCEPT program [11] equates a generalized creep strain, ε_g, and a generalized stress, σ_g, to longitudinal creep strain, ε_z, and longitudinal tensile stress, σ_z, occurring in a uniaxial creep test. Modeling of transient (primary) and

steady state (secondary) portions of the generalized creep curve as functions of temperature (T) and stress (σ_g) was by eq. (1) and eq. (2), respectively:

$$\dot{\varepsilon}_t = 2.13\times10^{9} \exp(-33200/T + .000113\ \sigma_g + .136\ \sigma_g/T)\ \varepsilon_t^{-1.50} \quad (1)$$

$$\dot{\varepsilon}_{ss} = 7.38\times10^{8} \exp(-23000/T)\ (\sinh 2.60 \times 10^{-10}\ \sigma_g^{2.28})^{.694} \quad (2)$$

Units required for input to the ACCEPT program are $\dot{\varepsilon}$ - hr^{-1}, σ_g - psi, and T - ^0K. Coefficients for this creep model were obtained from non-linear least squares fitting of logarithms of ε_t and ε_{ss} data from uniaxial tensile creep tests discussed above.

The DECAG thermal creep program investigated environments, loading conditions, and geometries very closely related to those of LWBR fuel rod plena. Two basic DECAG test specimen geometries were used: fixed axial gap and variable axial gap. Major parameters studied were axial gap length, radial gap (between cladding and Zircaloy plugs simulating thoria pellets and stainless steel plenum support sleeves), and temperature. Nominal outside diameter of the blanket cladding specimens was 1.443 cm. and nominal wall thickness was 0.066 cm. (Specimens were pickled to less than nominal LWBR standard blanket cladding thickness to be representative of minimum thickness cladding.)

Integral Zircaloy-4 end closures and inserts were machined to provide axial gaps ranging from 0.64 cm to 5.59 cm, and radial gaps of 0, 0.0038 cm, and 0.0089 cm. Fixed axial gap specimens were tested to investigate basic sensitivities to axial and radial gap sizes and to provide data used directly in qualifying analysis procedures. Additional specimens were tested with incrementally varied axial gap lengths to provide more realistic simulation of fuel rod experience.

Specimens were removed periodically from autoclaves for diameter measurements at mid-gap positions. Data were recorded as average outside diameter (average of maximum and minimum diameters) and ovality (difference between maximum and minimum diameters). The dominant deformation shape was two-lobed and approximately elliptical. Basic testing was conducted at 13.8 MPa and 357°C with comparison tests conducted at 336°C on selected specimens. Temperature in excess of LWBR blanket rod plenum environment was used to accelerate testing.

Data from the DECAG-II test program revealed (1) uniform shrinkage of unsupported cladding was relatively insensitive to axial gap length, (2) ovaling of unsupported cladding was a strong function of both gap length and radial clearance, (3) final ovality of specimens with axial gap lengths in the ranges tested was insensitive to initial ovality, and (4) variable axial gap specimens were more stable than fixed axial gap specimens with comparable initial radial gaps.

3. ACCEPT Analysis Program

The ACCEPT finite element computer program calculates elastic-plastic-creep deformation of Zircaloy tubes subjected to applied pressure, temperature, and axial force. Large deformation theory is used to accurately account for finite changes in geometry. Curved surfaces of the 20-node, tri-quadratic, isoparametic, 3-dimensional finite element allow accurate modeling of tube geometry, including such geometric imperfections as circumferential wall thickness variations and initial out-of-roundness. Capability to model frictionless contact-separation interaction of inner or outer surfaces of the tube with one or more rigid surfaces allows modeling of interaction between fuel rod cladding and fuel pellets.

Anisotropic behavior of Zircaloy and multi-axial loading of the cladding are accounted for with eq. (3), a modified version of Hill's model [15]. R, P, A, B, and C in eq. (3) are anisotropy coefficients. Strain rate in the i (r, θ, or z) coordinate direction is related to the generalized stress, σ_g, by the flow rule, eq. (4). Generalized creep rates, $\dot{\varepsilon}_g$, are calculated as functions of temperature and generalized stress by eq. (1) and eq. (2).

$$\sigma_g = \{[P(R+1)]^{-1}[R(\sigma_r-\sigma_\theta)^2 + RP(\sigma_\theta-\sigma_z)^2 + P(\sigma_z-\sigma_r)^2] + A\tau_{r\theta}^2 + B\tau_{\theta z}^2 + C\tau_{rz}^2\}^{1/2} \quad (3)$$

$$\varepsilon_i = \frac{\partial \sigma_g}{\partial \sigma_i} \dot{\varepsilon}_g(\sigma_g). \quad (4)$$

For LWBR fuel rod stability analysis, R was arbitrarily set at 1.35 and values of P and the shear anisotropy coefficients (A = B = C = 9.0) used in eq. (3) were derived from a fit of DECAG-II test specimen diameter changes and ovalities. Values of anisotropy coefficient P required in ACCEPT analysis were found to be correlated with initial radial gap. A small value of P (0.42) was required to predict deformation of zero radial gap specimens, and a large value of P (0.70) was required to predict deformation of specimens with 0.0089-cm radial gaps. P was varied linearly between 0.42 and 0.70 with initial radial gap in the range 0.0038 cm to 0.0147 cm. These anisotropy coefficients should be viewed as fitting parameters required to predict ovaling of biaxially loaded tubing and not as Zircaloy material properties; the variation of coefficient P accounts for unknown discrepancies in either the material model or the finite element program.

The finite element model used for variable axial gap test specimens is shown on Figure 1. Specimens were modeled using three-plane symmetry and initially elliptical cross section. Elongation of the axial gap was modeled by reducing multiple contact surface diameters to zero one at a time. The ACCEPT model for fuel rod plenum cladding uses a stationary support at the sleeve (top) end and multiple removable contact surfaces to model the moving pellet stack.

4. Calculated Test Specimen Ovalities

Figures 2 and 3 present detailed ACCEPT calculations for selected 0.0089-cm radial gap and 0.0038-cm radial gap, fixed axial gap specimens tested at 13.8 MPa and 357°C. The calculations are in good agreement with the measured ovalities. In particular, the axial gap length sensitivity of cladding ovality for both the 0.0089 and 0.0038-cm radial gap specimens is well calculated by ACCEPT. Because anisotropy coefficient P was selected to predict ovalities for specimens with differing end support radial gaps, the radial gap dependency of tubing ovality was well calculated also.

Figures 4 and 5 compare calculations of residual cladding ovality with data from two variable axial gap specimens tested. Tubing for one of these specimens was pre-ovaled to an initial value of 0.009 cm, whereas the other specimen had an as-fabricated ovality of .0013 cm. Residual ovalities of both specimens were well calculated, whereas diameter shrinkages (not shown) for both specimens were slightly undercalculated. As shown, ACCEPT calculates the observed reduction of cladding ovality early in test (when axial gap lengths were small) and the subsequent ovality increase as gap length was increased. Consistent with the test data, little difference in end of test performance of the pre-ovaled and the as-received tubing was calculated. In fact, because of larger initial end support clearances, the

specimen that was not pre-ovaled was calculated to have larger residual ovalities than the pre-ovaled specimen.

5. Sample Reactor Calculation

Figure 6 shows a sample calculation of cladding deformation over the plenum axial gap in a hypothetical reactor fuel rod (without pre-pressurization). The axial gap history and the modeled step approximation are shown. The reactor is operated at 13.8 MPa system pressure from 0 to 11,000 hours and at 12.4 MPa thereafter. For design analysis, it was assumed that bulk water boiling occurs in the plenum region of the fuel rod throughout life; therefore, T = 336°C between 0 and 11,000 hours, and T = 328°C beyond 11,000 hours. Best estimate bulk water temperatures are assumed to be 328°C between 0 and 11,000 hours and 316°C from 11,000 hours to 23,000 hours. The model included small allowances for fuel pellet diameter expansion and cladding loss due to corrosion.

On a best estimate basis, little deformation of the cladding is calculated to occur. On a design basis, which uses conservative values of geometry and creep parameters, collapse of the cladding is calculated to occur at about 21,500 hours of operation. The stepped approximation of axial gap growth results in some of the fictitious calculated ovality steps. However, actual step change in ovality would occur with the assumed reduction of system pressure at 11,000 hours.

References

[1] CONNORS, D. R, et al, "Design of the Shippingport Light Water Breeder Reactor," WAPD-TM-1208 (January 1979).

[2] GOLDBERG, I., et al, "Fission Gas Release from ThO_2 and ThO_2-UO_2 Fuels," WAPD-TM-1350 (August 1978).

[3] MOHR, C. L., "COVE-1, A Finite Difference Creep Collapse Code for Oval Fuel Pin Cladding Material," BNWL-1896 (March 1975).

[4] D. O. HOBSON, "Creepdown of Zircaloy Fuel Cladding - Initial Tests," ORNL/NUREG/TM-181 (April 1978).

[5] STEHLE, H., STEINBERG, E., and TENCKHOFF, E., "Mechanical Properties, Anisotropy and Microstructure of Zircaloy Canning Tubes," Zirconium in the Nuclear Industry, ASTM STP 633, A. L. Lowe, Jr. and G. W. Parry, Eds., American Society for Testing and Materials, pp. 486-500 (1977).

[6] MURTY, K. L., CLEVINGER, G. S., and PAPAZOGLOU, T. P., "Thermal Creep of Zircaloy-4 Cladding," Fourth Int'l Conf. on Structural Mechanics in Reactor Technology, San Francisco, Paper C3/4, 1977.

[7] BEAUREGARD, R. J., CLEVINGER, G. S., and MURTY, K. L., "Effect of Annealing Temperature on Mechanical Properties of Zircaloy-4 Cladding," Fourth Int'l Conf. on Structural Mechanics in Reactor Technology, San Francisco, Paper C3/5, 1977.

[8] SELSLEY, I. A., "Ex-Reactor Deformation of Externally Pressurized Short Lengths of Fuel Rod Cladding," WAPD-TM-1404 (May 1979).

[9] SELSLEY, I. A., "Externally Pressurized Thermal Creep Testing of Short Lengths of Zircaloy-4 Cladding," Trans. Am. Nucl. Soc. 33, pp. 267-270 (1979).

[10] SELSLEY, I. A., "Thermal Tests to Investigate Stability of Externally Pressurized Zircaloy-4 Tubing over Axial Gaps," WAPD-TM-1509 (July 1982).

[11] HUTULA, D. N., and WIANCKO, B. E., "ACCEPT: A Three-Dimensional Finite Element Program for Large Deformation Elastic-Plastic-Creep Analysis of Pressurized Tubes," WAPD-TM-1383 (March 1980).

[12] GORSCAK, D. A., and PFENNIGWERTH, P. L., "Analysis of Cladding Deformation over Plenum Axial Gaps in Zircaloy Clad Fuel Rods," WAPD-TM-1339 (December 1982).

[13] WOODS, C. R., et al, "Properties of Zircaloy-4 Tubing," WAPD-TM-585 (December 1966).

[14] EYLER, J. H., "The Characteristics of the Zircaloy-4 Tubing in LWBR Fuel Rods," WAPD-TM-869 (November 1979).

[15] R. HILL, "Yielding and Plastic Flow of Anisotropic Metals," Proc. Royal Society (London) 193A, pp. 281-297 (1948).

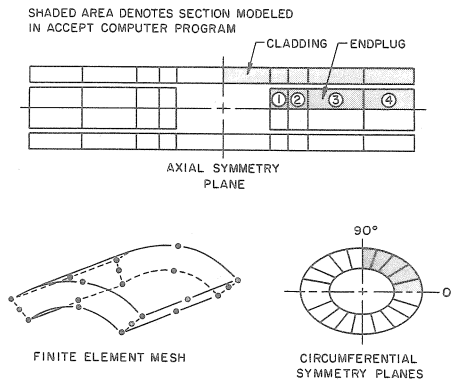

Figure 1. ACCEPT Finite Element Model for Variable Axial Gap Test Specimen

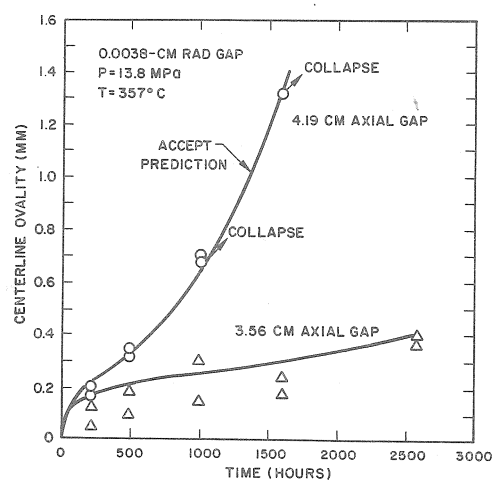

Figure 2. Residual Ovality for Selected 0.0038-cm Radial Gap, Fixed Axial Gap DECAG Specimens

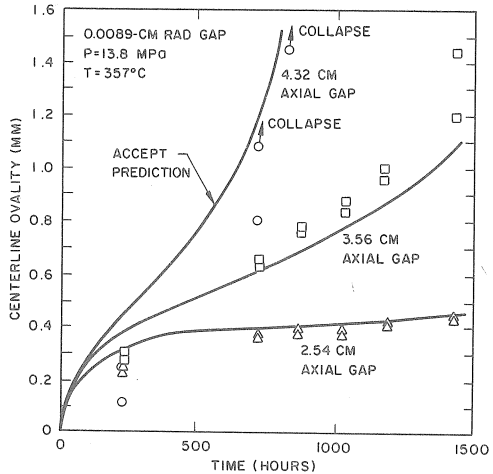

Figure 3. Residual Ovality for Selected 0.0089-cm Radial Gap, Fixed Axial Gap DECAG Specimens

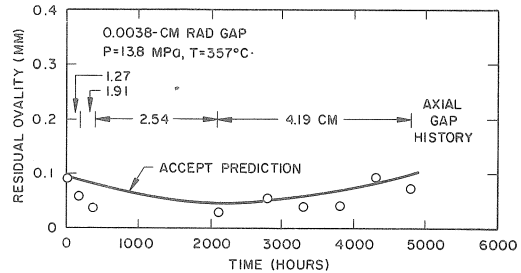

Figure 4. Residual Ovality: Pre-ovaled Variable Axial Gap Specimen

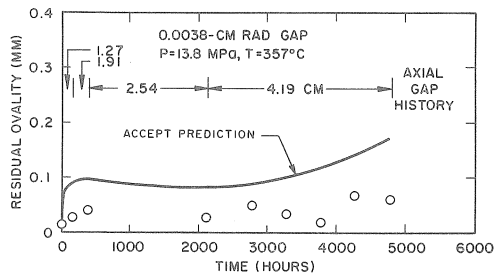

Figure 5. Residual Ovality: Small Initial Ovality Variable Axial Gap Specimen

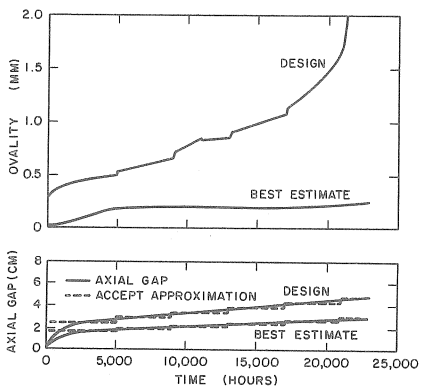

Figure 6. Sample Calculation of Ovality in Plenum of Reactor Fuel Rod